ADVANCED OPTICAL MATERIALS
www.advopticalmat.de

Origin of the Efficiency Roll-Off in Single-Layer Organic Light-Emitting Diodes Based on Thermally Activated Delayed Fluorescence

*Bas van der Zee, Yungui Li, Gert-Jan A. H. Wetzelaer, and Paul W. M. Blom**

The efficiency roll-off in organic light-emitting diodes (OLEDs) based on thermally activated delayed fluorescence (TADF) is attributed to either singlet–triplet or triplet–triplet annihilation (TTA) as well as triplet–charge annihilation. The origin of the efficiency roll-off on a TADF OLED consisting of a host-less single-layer emitter is studied. Varying the charge-carrier concentration at constant exciton density or the exciton density at constant charge-carrier density with temperature unambiguously shows that the dominant contribution to the roll-off originates from TTA. Using an analytical model, also the TTA rate constant can be obtained. These results show that single-layer TADF OLEDs are suited not only to determine the roll-off mechanism, but also to provide its rate constant directly from OLED efficiency measurements.

1. Introduction

The third generation of organic light-emitting diodes (OLEDs) utilizes emitters in which the splitting between the singlet and triplet excited states equals only several tens of meV. Thermal energy is then sufficient to convert triplet excitons to the emissive singlet state via reverse intersystem crossing (RISC) to attain a theoretical internal quantum efficiency (IQE) of 100% for electroluminescence.[1–3] This mechanism, termed thermally activated delayed fluorescence (TADF), has led to highly efficient OLEDs, and they are being considered as promising candidates in future display applications.[1] In practice, the maximum efficiency of a TADF OLED is commonly attained in the low-voltage regime at low brightness, while with increasing voltage the efficiency decreases.[4] This phenomenon is commonly known as "efficiency roll-off," and it is a negative effect as it reduces the efficiency at high light output. In addition to TADF OLEDs, also OLEDs with phosphorescent emitters suffer from efficiency roll-off.[5] For both types of OLEDs, the origin of the roll-off is a much debated topic, although triplet–triplet annihilation (TTA) and triplet–polaron quenching (TPQ) are the most commonly cited responsible mechanisms.[4–9] TTA has two possible outcomes: either one of the triplets (T_1) is lost (Equation (1))[10] or both triplets are lost, but a singlet exciton (S_1) is gained (Equation (2))

$$T_1 + T_1 \xrightarrow{3/4 * k_{TTA}} S_0 + T_1 \tag{1}$$

$$T_1 + T_1 \xrightarrow{1/4 * k_{TTA}} S_0 + S_1 \tag{2}$$

where S_0 is the singlet ground state and k_{TTA} is the TTA rate constant ($m^3\ s^{-1}$). We note here that we have omitted the formation of quintets, since the energy of the quintet state is typically higher than twice the triplet energy and therefore too high to be accessible at room temperature.[10–12]

The interaction between triplet excitons and polarons, TPQ,[5] leading to quenching of the T_1 state is represented as

$$T_1 + p/n \xrightarrow{k_{TPQ}} S_0 + p*/n* \tag{3}$$

where p/n is the hole/electron density (m^{-3}) and k_{TPQ} the triplet–polaron quenching constant ($m^3\ s^{-1}$). The asterisk indicates that after interaction with the triplet exciton, the polaron is in an excited state.

Another annihilation process that has been postulated to contribute to the efficiency roll-off in TADF OLEDs is singlet–triplet annihilation (STA).[6,7] It should be noted that in OLEDs with phosphorescent emitters STA is not significant due to the fast intersystem crossing (ISC) rate.[7] The STA reaction can be written as

$$S_1 + T_1 \xrightarrow{k_{STA}} S_0 + T_1 \tag{4}$$

with k_{STA} being the singlet–triplet annihilation constant. As can be seen, STA negatively impacts the singlet population, whereas TPQ and TTA affect the triplet population. In an OLED where all triplets are converted to radiative singlets, all these processes lead to a reduction of the efficiency.

The conventional way of investigating annihilation processes present in OLEDs is to measure the time decay of

B. van der Zee, Dr. Y. Li, Dr. G.-J. A. H. Wetzelaer, Prof. P. W. M. Blom
Molecular Electronics
Max Planck Institute for Polymer Research
Ackermannweg 10, 55128 Mainz, Germany
E-mail: blom@mpip-mainz.mpg.de

The ORCID identification number(s) for the author(s) of this article can be found under https://doi.org/10.1002/adom.202100249.

DOI: 10.1002/adom.202100249

photoluminescence (PL) and electroluminescence (EL). Subsequently, the transients are modeled with rate equations for the singlet as well as triplet population, from which the relevant quenching constants are then extracted.[4,13–15] The analysis is often complicated by dispersion effects, which can lead to time-dependent quenching constants.[16] A more straightforward approach would be to use the steady-state solutions of the rate equations, enabling the identification of annihilation processes directly from the measured OLED light output. This steady-state approach was applied to TADF OLEDs before, where both TTA and STA were incorporated in the rate equations for the singlet/triplet density to describe the efficiency roll-off.[6,17] In these studies, the roll-off analysis was performed on a multilayer architecture and with the TADF emitter doped in a host. Multilayer architectures are often adopted for their beneficial effect on the efficiency, but they strongly complicate a quantitative analysis of all the annihilation processes during device operation. For example, estimation of the carrier density in the emissive layer, required to analyze the role of TPQ, is not straightforward. Furthermore, the photophysical properties of the TADF emitters can vary widely depending on the choice of host,[18,19] such that the obtained TTA constant depends on the choice of host.[15] Ideally, a reliable steady-state analysis of the roll-off is performed in a model device using a single-layer architecture with an undoped emitter and nearly 100% IQE.

Such a highly efficient TADF OLED based on an undoped single-layer architecture was recently demonstrated with the emitter material, 9,10-bis(4-(9*H*-carbazol-9-yl)-2,6-dimethylphenyl)-9,10-diboraanthracene (CzDBA); its chemical structure is shown in **Figure 1**b.[20] CzDBA exhibits a photoluminescence quantum yield (PLQY) of >90% in film,[21] meaning that there is hardly any concentration quenching or nonradiative recombination via trap states. The latter stems from the fact that the lowest unoccupied molecular orbital (LUMO) and highest occupied molecular orbital (HOMO) levels of CzDBA, −3.45 and −5.93 eV respectively,[20] are situated close to the so-called trap-free window,[22] which ranges from −3.6 to −6.0 eV with respect to the vacuum level, resulting in near trap-free electron and hole transport.[20] The absence of internal losses and balanced transport gives rise to high external quantum efficiency (EQE) values of 19% at 500 cd A^{-1},[20,23] meaning that for ≈20% light-outcoupling efficiency an IQE of ≈95% is attained in the single-layer CzDBA OLED. Single-layer OLEDs based on CzDBA therefore form an ideal model system to investigate the efficiency roll-off in TADF OLEDs. In the present study, we examine the voltage and temperature dependence of the external quantum efficiencies of CzDBA OLEDs. Using steady-state solutions of the rate equations for STA, TTA, and TPQ, we demonstrate that TTA is the dominant mechanism in the efficiency roll-off in our TADF OLEDs. Our analytical formulas provide a facile way to identify the roll-off mechanism and the corresponding annihilation rate directly from the OLED efficiency.

2. Results and Discussion

The fabrication of a CzDBA OLEDs was outlined previously and leads to the device structure presented in Figure 1b.[20] In short,

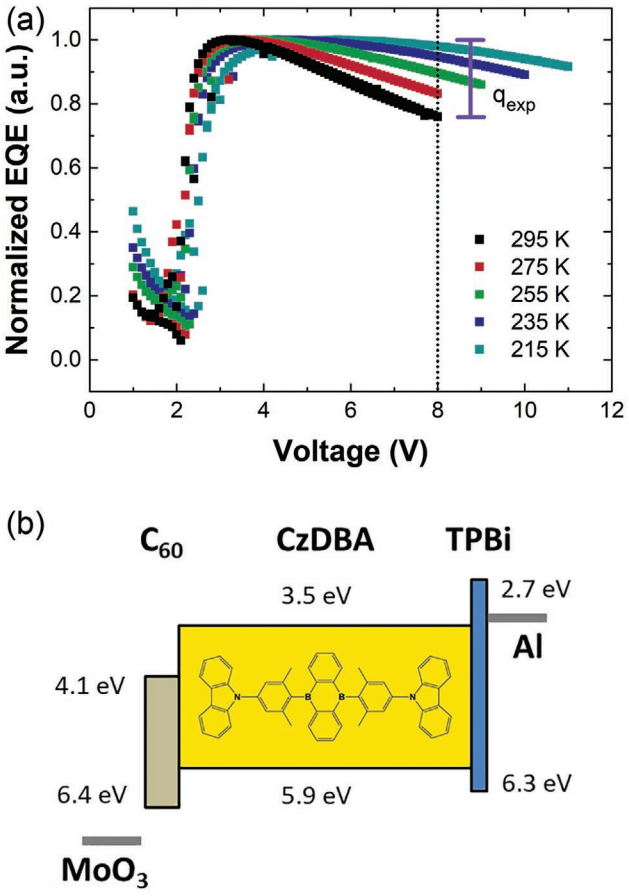

Figure 1. a) Normalized temperature-dependent external quantum efficiency versus voltage for a 300 nm CzDBA OLED. The experimental quenching parameter q_{exp} is indicated graphically. b) Schematic band diagram showing the device layout of a CzDBA OLED, the chemical structure of CzDBA is shown in the emissive layer. The HOMO/LUMO levels are given (f.l.t.r.) for C_{60}, CzDBA, and TPBi (2,2′,2″-(1,3,5-benzinetriyl)-tris(1-phenyl-1-H-benzimidazole)).[20]

a thick (300 nm) CzDBA layer is sandwiched between Ohmic electron and hole contacts enabled by tunneling interlayers.[20] Figure 1a shows the normalized EQE versus voltage for a 300 nm CzDBA OLED at various temperatures. Going from 295 to 215 K we observe a flatter efficiency curve in combination with a shift of the maximum efficiency from 3.2 to 5.7 V. Considering one specific voltage, namely 8 V as indicated by the dotted line in Figure 1a, it can be seen that the efficiency increases with decreasing temperature. From single carrier devices it has been demonstrated that CzDBA exhibits low trap concentrations for both electrons and holes.[20] As a result, it was shown that already for an applied voltage of only 1.0–1.5 V the traps are nearly all filled. For the CzDBA OLED, this automatically means that for a voltage of 1.0–1.5 V above the build-in voltage (≈2.0 V), so typically a voltage larger than 3.5 V, the OLED operates in the trap-filled limit, where the current is space-charge limited. Furthermore, recombination is mainly governed by the bimolecular Langevin recombination, since, due to the low amount of traps, trap-assisted recombination does not play a role at higher voltages. This is further evidenced by comparing the experimental OLED current with the analytical model for double-carrier

injection into a trap-free material with bimolecular recombination as a dominant recombination mechanism.[24] As shown in Section S2 (Supporting Information) the excellent agreement between the experiment and model confirms that this OLED mainly operates in the trap-free space-charge-limited regime, which implies that the carrier densities are governed by the applied voltage only, nearly independent of temperature. By cooling down the OLED, both the current and luminance at 8 V therefore drop due to the decrease of the carrier mobility with temperature, whereas the carrier density remains nearly constant. As a result, the quenching parameter q_{exp} (Figure 1a), defined as $q_{exp} = 1 - \eta_{exp}$ with η_{exp} being the normalized experimental efficiency, is only affected by a change in exciton density. The decrease of q_{exp} with decreasing temperature therefore indicates that excitons are involved in the quenching. Complementing the efficiency analysis at constant voltage, the efficiency can also be examined as a function of current density, as shown in **Figure 2**. At constant current density the light output remains nearly constant, while the operating voltage and, thus, carrier density increase with decreasing temperature due to the temperature-dependent mobility. Consequently, a change in exciton quenching would be mainly governed by a change in carrier density in this case. Figure 2 shows that at one specific current density (20 A m^{-2}), as indicated by the dotted line, the efficiency, and thus quenching, is almost temperature invariant. This indicates that charge carriers or polarons do not play an important role in the quenching process.

As a next step, we derive the steady-state solutions of the singlet and triplet concentrations for the various quenching mechanisms, starting with triplet–triplet annihilation. The rate equation of the singlet population is given by

$$\frac{d[S]}{dt} = 0.25 \cdot G - \frac{[S]}{\tau_s} + k_{RISC} \cdot [T] = 0 \quad (5)$$

which gives a relation between the singlet exciton density $[S]$ and triplet density $[T]$.

The triplet density $[T]$ is derived from the rate equation for triplets

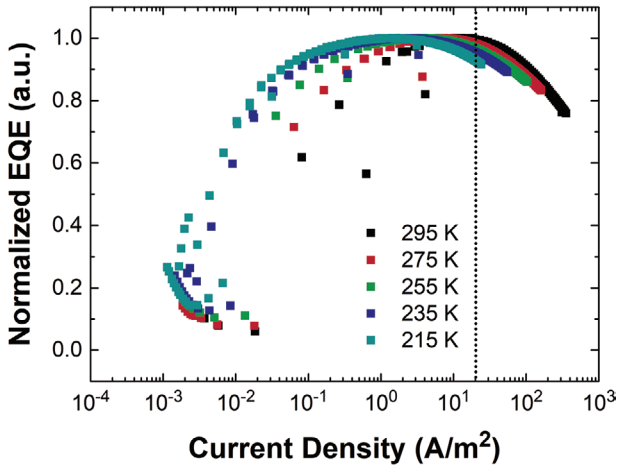

Figure 2. Normalized efficiency versus current density for temperatures ranging from 295 to 215 K in steps of 20 K. The dotted line indicates the efficiency at a current density of 20 A m^{-2}.

$$\frac{d[T]}{dt} = 0.75 \cdot G - \frac{[T]}{\tau_t} - k_{RISC} \cdot [T] - k_{TTA} \cdot [T] \cdot [T] = 0 \quad (6)$$

In these equations, τ_s/τ_t is the singlet/triplet lifetime and G is the exciton generation rate. We assume uniform generation over the emission layer due to the balanced transport, such that we can write $G = \frac{J}{q \cdot d}$, with J being the current density, q the elementary charge, and d the emitter layer thickness. In these equations, we make use of the fact that our TADF OLED is mainly loss free with an IQE close to unity. In this case, almost all triplets eventually undergo a spin flip to the singlet state to give fluorescence. As a first step, we assume that intersystem crossing does not affect the final steady-state singlet and triplet concentrations, and thus is for now it is omitted in the rate equations. Furthermore, we assume that TTA only affects the triplet population (Equation (1)). The singlet generation from TTA (Equation (2)) has a prefactor of only 0.25, whereas the total prefactor of triplet disappearance is 1.25. Moreover, the dominant contribution to the singlet population is not expected to be from TTA, but from RISC instead.[4] The last assumption we make is that the intrinsic triplet lifetime is long enough such that the monomolecular decay of triplets can be neglected, which agrees with an IQE near unity. This is implemented by $\tau_t \to \infty$. Typical triplet lifetimes are on the order of at least 100 µs,[25] much longer than the effective triplet lifetime that is dominated by RISC. The effective triplet lifetime for CzDBA was determined to be 3.2 µs at room temperature.[21] Combining Equations (5) and (6) we obtain an analytical expression for the normalized efficiency (η_{TTA}) in case of TTA (full derivation is given in the Supporting Information), given by

$$\eta_{TTA} = 0.25 + \frac{k_{RISC}^2}{2k_{TTA} \cdot G}\left(-1 + \sqrt{1 + \frac{4k_{TTA} \cdot 0.75G}{k_{RISC}^2}}\right) \quad (7)$$

The first term in Equation (7) represents the direct generation of singlets, which under electrical operation are produced in a singlet-to-triplet ratio of 1:3. The second term describes the singlets generated by RISC. We note that if $4k_{TTA} \cdot 0.75G/k^2_{RISC} \ll 1$ the η_{TTA} approaches unity using the binomial approximation $\left(\sqrt{1+x} \approx 1 + \frac{1}{2}x\right)$.

Following the same approach, expressions for the normalized OLED efficiency can also be derived in case of STA and TPQ, given by (Section S1, Supporting Information)

$$\eta_{STA} = \frac{\frac{[S]}{\tau_s}}{G} = \frac{1}{1 + \frac{k_{STA}\,\tau_s \cdot 0.75G}{k_{RISC}}} \quad (8)$$

and

$$\eta_{TPQ} = \frac{\frac{[S]}{\tau_s}}{G} = 0.25 + \frac{k_{RISC}}{k_{RISC} + k_{TPQ} \cdot (n+p)} \quad (9)$$

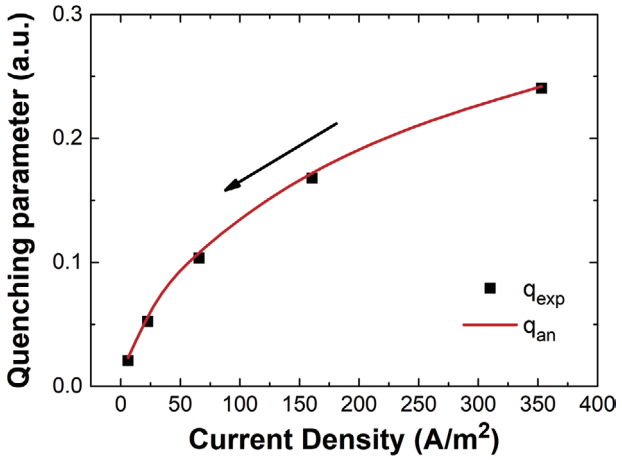

Figure 3. Experimental quenching parameter q_{exp} as a function of current density at 8 V (symbols). The arrow indicates the direction of decreasing temperature from 295 to 215 K in steps of 20 K. Also shown is the calculated roll-off (analytical quenching parameter, q_{an}) for TTA as quenching mechanism using Equation (7) with $k_{TTA} = 1.2 \times 10^{-17}$ m^{-3} s^{-1} (solid line). This solid line serves as a guide to the eye and was obtained by interpolating the values of q_{an} with a cubic spline.

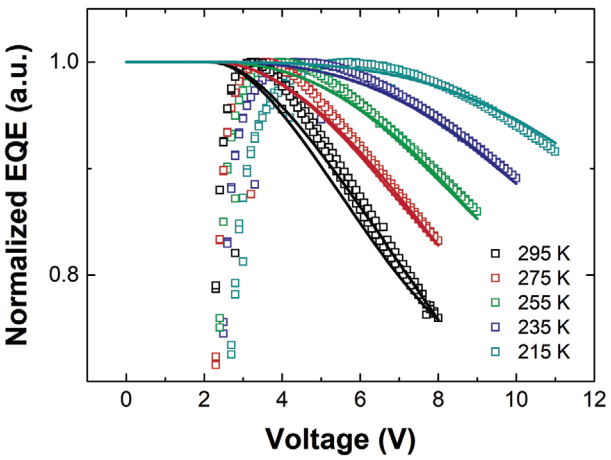

Figure 4. Normalized efficiency versus voltage for a 300 nm CzDBA OLED (symbols) complemented by fits to Equation (7) (lines) considering TTA as exciton quenching mechanism. For all fits a rate constant k_{TTA} of 1.2×10^{-17} m^3 s^{-1} has been used.

As a next step, these steady-state solutions of the rate equations are compared with the experimentally observed efficiency roll-off. In **Figure 3**, the quenching parameter q_{exp} is plotted as a function of the current density at a constant voltage of 8 V (symbols).

We observe that at room temperature the roll-off losses due to exciton quenching amount to 24% at 8 V, whereas at 215 K the losses have been reduced to 2% only.

For the case of TTA the normalized efficiency η_{TTA} depends on G, k_{RISC}, and k_{TTA} (Equation (7)). The generation rate is directly obtained from the OLED current density J which is known as a function of voltage and temperature. Furthermore, for CzDBA, k_{RISC} was determined to be 3.13×10^5 s^{-1} at room temperature with a thermal activation energy of 33 meV,[21] such that k_{RISC} is known at any temperature. As a result, k_{TTA} is the only free parameter for describing the efficiency roll-off due to TTA. By setting k_{TTA} to a fixed value of 1.2×10^{-17} m^3 s^{-1}, independent of temperature, we obtain excellent agreement between the experiment and the model for TTA. The obtained magnitude for k_{TTA} is in the range of earlier reported values obtained via transient methods, typically from $\approx 10^{-17}$ to $\approx 10^{-20}$ m^3 s^{-1}.[4,16,17]

In contrast, in the model for TPQ (Equation (9)) at constant voltage, p and n are fixed and the only contribution from temperature comes in via k_{RISC} and/or k_{TPQ}. The known variation of k_{RISC} is not strong enough to explain the decrease of q_{exp} with current density and/or temperature, meaning that a strong temperature dependence of k_{TPQ} would be required to explain the reduced quenching at low temperatures. However, as already indicated by the temperature-independent quenching at a fixed current (Figure 2), charge-carrier density and, therefore, TPQ do not seem to play an important role in the efficiency roll-off of the TADF OLED. From the three quenching mechanisms considered, only TTA reproduces the square-root like dependence of q_{exp} on current density/generation rate.

Having investigated the roll-off at a fixed voltage we now further establish the dominant quenching mechanism by considering the full voltage range. **Figure 4** shows the experimental and calculated normalized efficiency versus voltage for a 300 nm CzDBA OLED, considering TTA as the dominant quenching mechanism. The efficiency decrease with voltage at room temperature is well described using a rate constant k_{TTA} of 1.2×10^{-17} m^3 s^{-1}. Since the temperature dependence of G and k_{RISC} is known, the roll-off for all other temperatures can be predicted using (Equation (7)) combined with this value for k_{TTA}.

We observe that with this fixed k_{TTA} value, the voltage dependence of the efficiency roll-off at all temperatures is consistently described, confirming the dominance of TTA as the cause of the efficiency roll-off. The slight deviation at voltages just above the build-in voltage (≈2 V at 295 K) stems from the trap filling of the small amount of electron and hole traps that are present in this material.[20] Our model is intended to study the roll-off in the trap-filled limit (>3.5 V) and does not consider the details of trapping at low voltages. Since at low temperatures the roll-off shifts to higher voltages (>4 V), the agreement gets better since at higher voltages trapping does not play a role, as discussed before.

The observation that the roll-off at any temperature can be described by a fixed temperature-independent k_{TTA} is surprising. In order to rationalize this experimental finding, we note that, in recent kinetic Monte Carlo simulations of the TTA process,[26] it was found that in the relatively small temperature range of our study (215–295 K) the temperature dependence of TTA is weak, providing that the energetic disorder is small. Since in CzDBA the electron and hole transports are trap free and exhibit a high mobility, indicative of low energetic disorder, we suggest that the reduced disorder in combination with the limited experimental temperature regime might be the cause of our observation of a nearly temperature-independent k_{TTA}.

One could argue that the temperature dependence of q_{exp} at a fixed voltage can also arise from a strong temperature dependence of k_{TPQ}. However, even with k_{TPQ} as a fit parameter at

every temperature, the functional form of the voltage dependence of the roll-off cannot be described (Figure S2a, Supporting Information). For STA, the voltage dependence of the quenching process can be reasonably reproduced using a temperature-dependent k_{STA} (Figure S2b, Supporting Information). However, to explain the quenching at room temperature and anomalously high rate constant k_{STA} of 1×10^{-15} m^3 s^{-1} has to be used, three orders of magnitude higher than previously reported.[4] Furthermore, to describe the quenching at lower temperatures, k_{STA} would have to be further increased, ruling out the occurrence of this process. Consequently, by simply measuring the current density and light output of the OLED as a function of voltage, which together give the efficiency, the mechanism, and magnitude of the quenching process, can be directly obtained from a comparison with the analytical models.

So far, we have demonstrated that the experimentally observed roll-off of the single-layer TADF OLED is well described by the TTA process with a rate constant k_{TTA} of 1.2×10^{-17} m^3 s^{-1}. However, it should be noted that this was obtained ignoring the effect of the ISC process. It is expected that the omission of ISC has a major impact on the determination of the k_{TTA} value. Due to ISC, more triplets will be formed than we consider until now. This increased triplet population than results in a decreasing k_{TTA} in order to model the same roll-off. As the next step we incorporate ISC in the rate equations in order to derive a modified expression for the OLED efficiency. Including ISC the OLED efficiency is given by

$$\eta_{TTA,ISC} = \frac{1}{G} \frac{0.25 \cdot G + k_{RISC} \cdot [T]}{\tau_s^{-1} + k_{ISC}} \tag{10}$$

with $[T]$ being

$$[T] = -\frac{k_{RISC}}{2\left(k_{TTA} + k_{TTA} \cdot k_{ISC} \cdot \tau_s\right)} + \sqrt{\frac{1}{4} \cdot \left(\frac{k_{RISC}}{k_{TTA} + k_{TTA} \cdot k_{ISC} \cdot \tau_s}\right)^2 + \frac{0.75 \cdot G + k_{ISC} \cdot \tau_s \cdot G}{k_{TTA} + k_{TTA} \cdot k_{ISC} \cdot \tau_s}} \tag{11}$$

The derivation for this expression can be found in Section S1 (Supporting Information). Assuming an ISC rate[21] of 3.8×10^7 s^{-1} we remodel the efficiency decrease of the CzDBA OLED at $T = 295$ K using Equation (10). As shown in **Figure 5**, where we plot the normalized efficiency versus voltage, comparing the analytical models with and without ISC, we find that including ISC lowers the TTA rate constant by an order of magnitude to 1.5×10^{-18} m^3 s^{-1}, whereas the functional dependence of the roll-off on voltage remains invariant. A rate constant k_{TTA} in the 10^{-18} m^3 s^{-1} regime is therefore more realistic.

A big advantage of studying the effect of TTA on the roll-off in a single-layer OLED is that due to the simple device architecture the amount of injected carriers and excitons formed can be easily obtained, facilitating a quantitative analysis. Since the charge transport of CzDBA is almost balanced,[20] the recombination zone is spread over the thickness of the emissive layer. In contrast, in multilayer OLEDs, the excitons are confined in a small volume. Confinement leads to more interaction between the excitons, and one could thus expect a stronger effect of TTA on the roll-off. However, another difference between the two architectures is that in a multilayer device the emitters are incorporated in a host, which will hinder the interaction between triplet excitons. These two competing processes make the study of the roll-off more complex in a multilayer OLED. Furthermore, due to the presence of many layers with various energy offsets, the carrier density and exciton formation in the emissive part of the multilayer OLED are not easily determined. Therefore, our analysis of the roll-off, although more straightforward, cannot directly be extended to multilayer OLEDs with a host–guest emissive layer.

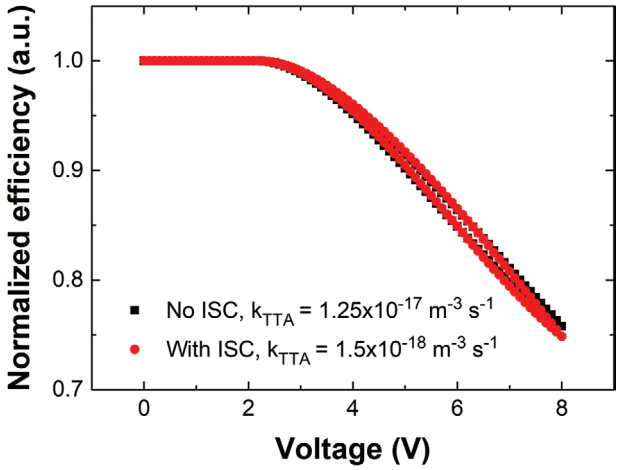

Figure 5. Normalized efficiency versus voltage comparing Equation (7) (model without ISC) and Equation (10) (model with ISC) for 295 K.

3. Conclusion

Summarizing, we have investigated the efficiency roll-off using a single-layer model TADF OLED based on the emitter CzDBA, in which the influence of a host and/or a multilayer architecture do not obstruct a reliable analysis. By assessing the temperature-dependent efficiency at a fixed voltage, we find that the roll-off changes drastically. Opposite to this, the temperature-dependent efficiency shows little change for a fixed current density. Combination of these observations shows that the efficiency roll-off of the TADF OLED is not caused by charge carriers, but originates from excitonic processes. Analytical formulas for the efficiency are derived in the case the roll-off is ascribed to either STA, TTA, or TPQ. By comparison with the experiment we are able to discern between these different possible causes of the roll-off, pointing to TTA as the dominant mechanism. TTA is not only able to describe the efficiency loss at only one voltage, but the entire voltage range is very well described by the analytical formula presented here. As a last point of discussion, a more realistic case is presented, where ISC is included in the rate equations. It shows that an accurate determination of the triplet population will only alter the magnitude of the triplet–triplet annihilation constant, not the shape of the efficiency curve. As a result, the use of these analytical formulas provides a quick estimate of the quenching mechanism and corresponding rate constant from standard OLED characterization techniques.

Supporting Information

Supporting Information is available from the Wiley Online Library or from the author.

Acknowledgements

Open access funding enabled and organized by Projekt DEAL.

Conflict of Interest

The authors declare no conflict of interest.

Data Availability Statement

The data that support the findings of this study are available from the corresponding author upon reasonable request.

Keywords

device physics, efficiency roll-off, organic light-emitting diodes, triplet–triplet annihilation

Received: February 3, 2021
Revised: May 10, 2021
Published online: June 19, 2021

[1] Y. Liu, C. Li, Z. Ren, S. Yan, M. R. Bryce, *Nat. Rev. Mater.* **2018**, *3*, 18020.
[2] H. Uoyama, K. Goushi, K. Shizu, H. Nomura, C. Adachi, *Nature* **2012**, *492*, 234.
[3] K. Goushi, K. Yoshida, K. Sato, C. Adachi, *Nat. Photonics* **2012**, *6*, 253.
[4] M. Hasan, A. Shukla, V. Ahmad, J. Sobus, F. Bencheikh, S. K. M. McGregor, M. Mamada, C. Adachi, S.-C. Lo, E. B. Namdas, *Adv. Funct. Mater.* **2020**, *30*, 2000580.
[5] C. Murawski, K. Leo, M. C. Gather, *Adv. Mater.* **2013**, *25*, 6801.
[6] K. Masui, H. Nakanotani, C. Adachi, *Org. Electron.* **2013**, *14*, 2721.
[7] A. Niwa, S. Haseyama, T. Kobayashi, T. Nagase, K. Goushi, C. Adachi, H. Naito, *Appl. Phys. Lett.* **2018**, *113*, 083301.
[8] Y. Zhang, S. R. Forrest, *Phys. Rev. Lett.* **2012**, *108*, 267404.
[9] S. Reineke, K. Walzer, K. Leo, *Phys. Rev. B* **2007**, *75*, 125328.
[10] A. Köhler, H. Bässler, *Mater. Sci. Eng., R* **2009**, *66*, 71.
[11] B. Dick, B. Nickel, *Chem. Phys.* **1983**, *78*, 1.
[12] D. Y. Kondakov, T. D. Pawlik, T. K. Hatwar, J. P. Spindler, *J. Appl. Phys.* **2009**, *106*, 124510.
[13] S. Reineke, G. Schwartz, K. Walzer, M. Falke, K. Leo, *Appl. Phys. Lett.* **2009**, *94*, 163305.
[14] M. A. Baldo, C. Adachi, S. R. Forrest, *Phys. Rev. B* **2000**, *62*, 10967.
[15] D. Kasemann, R. Brückner, H. Fröb, K. Leo, *Phys. Rev. B* **2011**, *84*, 115208.
[16] L. Zhang, H. van Eersel, P. A. Bobbert, R. Coehoorn, *Chem. Phys. Lett.* **2016**, *652*, 142.
[17] M. Inoue, T. Sereviius, H. Nakanotani, K. Yoshida, T. Matsushima, S. Juršnas, C. Adachi, *Chem. Phys. Lett.* **2006**, *644*, 62.
[18] K. Stavrou, L. G. Franca, A. P. Monkman, *ACS Appl. Electron. Mater.* **2020**, *2*, 2868.
[19] G. Méhes, K. Goushi, W. J. Potscavage, C. Adachi, *Org. Electron.* **2014**, *15*, 2027.
[20] N. B. Kotadiya, P. W. M. Blom, G. A. H. Wetzelaer, *Nat. Photonics* **2019**, *13*, 765.
[21] T. L. Wu, M. J. Huang, C. C. Lin, P. Y. Huang, T. Y. Chou, R. W. Chen-Cheng, H. W. Lin, R. S. Liu, C. H. Cheng, *Nat. Photonics* **2018**, *12*, 235.
[22] N. B. Kotadiya, A. Mondal, P. W. M. Blom, D. Adrienko, G. A. H. Wetzelaer, *Nat. Mater.* **2019**, *18*, 1182.
[23] W. Liu, N. B. Kotadiya, P. W. M. Blom, G. A. H. Wetzelaer, D. Andrienko, *Adv. Mater. Technol.* **2021**, *6*, 2000120.
[24] L. M. Rosenberg, M. A. Lampert, *J. Appl. Phys.* **1970**, *41*, 508.
[25] O. V. Mikhnenko, P. W. M. Blom, M. A. Loi, *Phys. Chem. Chem. Phys.* **2011**, *13*, 14453.
[26] R. Saxena, T. Meier, S. Athanasopoulos, H. Bässler, A. Köhler, *Phys. Rev. Appl.* **2020**, *14*, 034050.